Renewable Energy 36 (2011) 2959–2966

Contents lists available at ScienceDirect

Renewable Energy

journal homepage: www.elsevier.com/locate/renene

# Thermal and rheological properties of microencapsulated phase change materials

G.H. Zhang [a], C.Y. Zhao [a,b,*]

[a] School of Engineering, University of Warwick, Coventry, CV4 7AL, UK
[b] School of Mechanical Engineering, Shanghai Jiaotong University, Shanghai 200240, China

ARTICLE INFO

*Article history:*
Received 14 December 2010
Accepted 1 April 2011
Available online 7 May 2011

*Keywords:*
MPCM
MPCS
Thermal properties
Rheological properties
Heat transfer

ABSTRACT

The use of microencapsulated phase change materials (MPCMs) is one of the most efficient ways of storing thermal energy. When the microencapsulated phase change material (MPCM) is dispersed into the carrier fluid, microencapsulated phase change slurry (MPCS) is prepared. Due to the relatively large surface area to volume MPCM and its large apparent specific heat during the phase change period, better heat transfer performance can be achieved. Therefore, MPCS can be used as both the energy storage and heat transfer media.

This paper studies the thermal and rheological properties of a series of prepared MPCS. In the experiment: MPCS fabricated by dispersing MPCM into water with an appropriate amount of surfactant. The mass ratio of MPCM to water and surfactant was 10:90:1, 25:75:1, 35:65:1 in prepared MPCS samples, respectively. Then the thermal conductivity and specific heat of MPCS were measured by the Hot Disk. The melting/crystallizing temperature and fusion heat/crystallization heat of the phase change materials were obtained from a DSC (differential scanning calorimetry) during the heating/cooling process. Physical properties, such as viscosity, diameter and its size distribution of MPCS were investigated by a rheometer and a particle characterization system. Meanwhile, the chemical structure of the sample was analyzed using Fourier Transformed Infrared spectroscopy (FTIR).

The results showed that the thermal conductivity and the specific heat of MPCS decreased with particle concentration for the temperatures below the melting point. Overall, the MPCS can be considered as Newtonian fluid within the test region (shear rate $>200\ s^{-1}$ and mass fraction $<0.35$). The viscosity is higher for bigger particle slurries. The findings of the work lead to the conclusion that the present work suggested that MPCMs can be used in "passive" applications or in combination with active cooling systems; and it also provided a new understanding for fabricating microencapsulated phase change slurry, it is for sure that to have a better potential for energy storage. Accordingly, it has demonstrated that the MPCS fabricated in the current research are suitable for potential application as heat transfer media in the thermal energy storage.



## 1. Introduction

Phase change materials (PCMs) have long been used for thermal energy storage due to the large amount of heat absorption/release while undergoing phase changes, with only small temperature variations [1–10]. Organic and inorganic materials are two most common groups of PCMs [11]. Organic materials are further described as paraffin and non-paraffin. Most organic PCMs are non-corrosive and chemically stable, and have little or no sub-cooling. They are compatible with most building materials and have a high latent heat per unit weight and low vapour pressure. But they also have disadvantages in low thermal conductivities, high changes in volume on phase change and flammability. In contrast, inorganic materials (salt hydrate and metallic) have a high latent heat per unit volume and high thermal conductivities, and are non-flammable and low in cost in comparison to organic materials. However, they are corrosive to most metals and suffer from decomposition and sub-cooling, which can affect their phase change properties. Therefore, In order to overcome these problems, a new technique of utilizing microencapsulated phase change material (MPCMs) in thermal energy storage system has been developed. Microencapsulated PCMs provide a means to solve the supercooling problem and interfacial combination with the circumstance materials [12]. The main merits of microencapsulated

* Corresponding author. School of Engineering, University of Warwick, Coventry, CV4 7AL, UK. Tel.: +44 (0) 24 76522339.
*E-mail addresses:* C.Y.Zhao@warwick.ac.uk, changying.zhao@sjtu.edu.cn (C.Y. Zhao).

0960-1481/$ – see front matter © 2011 Elsevier Ltd. All rights reserved.
doi:10.1016/j.renene.2011.04.002

**Nomenclature**

| | |
|---|---|
| $C_p$ | specific heat capacity (kJ/(kg °C)) |
| $d$, $D$ | diameter (m) |
| $\Delta H_c$ | heat of crystallization (kJ/kg) |
| $\Delta H_f$ | heat of fusion (kJ/kg) |
| $k$ | Thermal conductivity (W/(m °C)) |
| $m$ | mass (kg) |
| $T_m$ | melting temperature (°C) |
| $T_c$ | crystallizing temperature (°C) |
| $W$ | mass fraction (–) |

*Greek letters*

| | |
|---|---|
| $\rho$ | density (kg/m$^3$) |
| $\Phi$ | the encapsulation efficiency (%) |
| $\mu$ | viscosity (Pa s) |

*Subscripts*

| | |
|---|---|
| $b$ | bulk |
| $c$ | microcapsule core |
| $f$ | fluid |
| $p$ | particle |
| $w$ | wall, water |

phase change material (MPCM) over PCM are as follows: (1) increasing heat transfer area; (2) reducing PCMs reactivity toward the outside environment and controlling the changes in the storage material volume as phase change occurs. The use of microencapsulated phase change materials (MPCMs) is one of the most efficient ways of storing thermal energy and it has received a growing attention in the past decade [12–27]. Since MPCM was developed, it had been mainly used in the textile [19,28–31] and building applications [32–36].

Due to the low thermal conductivity of PCMs [10], a new approach was proposed to improve the thermal performance of the thermal system (e.g. the secondary refrigeration and air conditioning loops). When the MPCM is dispersed into the carrier fluid, e.g. water, a kind of suspension named as microencapsulated phase change material slurry (MPCS) is formed [37]. Water is normally used as the carrier fluid since it has no obvious negative effect on fabricating MPCS and is cheap to get, although the carrier fluid should have a high thermal conductivity and a large specific heat capacity. In comparison of conventional phase change material slurries (PCS), better heat transfer performance can be achieved due to the relatively large surface area to volume of MPCM. Therefore, it can be used as both thermal energy storage and heat transfer media [38–43]. The thermal and physical properties of MPCS are crucial for the MPCS system design, and they are very different from those of the MPCM materials and carrier fluids. These mainly include the thermal conductivity, viscosity and specific heat. The optimum design of thermal energy storage systems, which run with microencapsulated phase change material slurry, requires a good knowledge of flow and heat transfer characteristics of two-phase slurry involved in phase change, in order to reduce the capital cost, system size, and energy consumption [44].

The purpose of this study is to investigate the thermal and rheological properties of the MPCMs. In this paper, a series of MPCS were prepared for experimental test. The chemical structure, morphology, microstructure, diameter and its size distribution, thermal properties of the MPCMs and rheological properties of MPCS were obtained from experimental measurements.

## 2. Experimental test

### 2.1. Investigated materials

- DPNT06-0182 (Ciba Specialty Chemicals, UK), properties of microcapsule as given by the manufacture: it comprises 87.5% paraffin wax and 12.5% crosslinked acrylic polymer shell (core/shell ratio: 87.5:12.5).
- Micronal® DS 5008X (BASF, Germany), properties of microcapsule as given by the manufacture: it comprises a paraffin mixture and highly crosslinked polymethyl methacrylate (PMMA) shell; formaldehyde-free (core/shell ratio: 7:3).

### 2.2. Chemical composite analysis

The chemical structure was analyzed using PerkinElmer-Spectrum 100 Fourier transformed infrared spectroscopy (FTIR) with the KBr sampling method.

### 2.3. Surface morphology and structure of microcapsules

Morphologies were obtained by using a Cambridge instruments-STEREOSCAN 90 scanning electron microscopy (SEM). A Reichert Jung–Polyvar MET optical phase-contrast microscope was employed to investigate the microstructure of the microcapsules.

### 2.4. Diameter measurement

The microcapsules size distribution from light diffraction was performed using a Malvern Instruments-Hydro 2000S laser particle size analyzer, and the mean diameters of the microcapsules were determined.

### 2.5. Thermal properties of microcapsules

Differential scanning calorimetry (DSC) was performed to determine the melting temperature and heat of fusion during the heating process, crystallizing temperature and crystallization heat during the cooling process by using a SETARAM Instrumentation-D/SENSYS-2A differential scanning calorimeter, and all measurements were carried out under an air atmosphere at a heating or cooling rate of 0.2 °C/min. Thermal gravimetry (TG) analysis was applied to measure the thermal stability of these microcapsules by a Polymer laboratories-STA 1500. The Thermal conductivity and specific heat of the MPCMs and MPCS were tested by using a Hot Disk

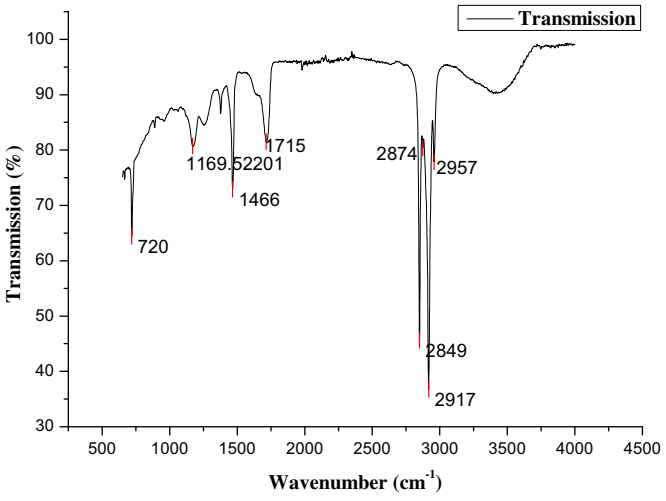


**Fig. 1.** FTIR spectra of microPCMs (DPNT06-0182 CIBA).

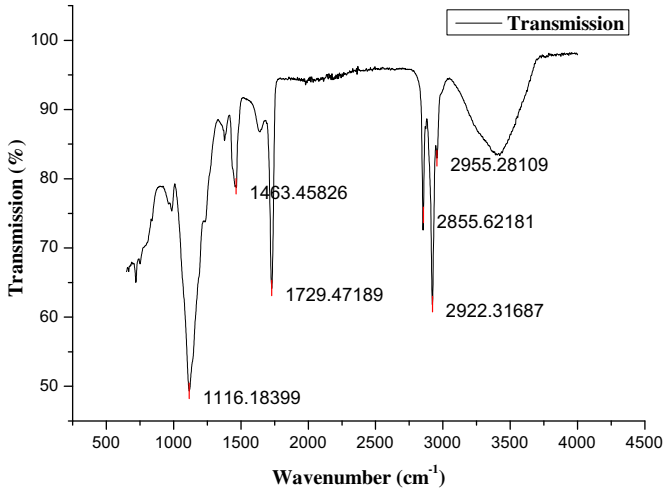


**Fig. 2.** FTIR spectra of microPCMs (DS 5008X BASF).

Instruments-TPS 2500S. The following sets of thermal property models that used by previous researchers to MPCS were employed in this study.

The density & specific heat of the microcapsules and the specific heat of MPCS were calculated using mass and energy balance [38]:

$$\rho_p = \frac{\text{Microcapsule mass}}{\text{core mass}}\left(\frac{d_c}{d_p}\right)^3 \rho_c \tag{1}$$

$$C_{P,P} = \frac{(\text{Core mass}\cdot C_c + \text{Shell mass}\cdot C_w)\rho_c\rho_w}{(\text{Shell mass}\cdot \rho_c + \text{Core mass}\cdot \rho_w)\rho_p} \tag{2}$$

$$C_{P,b} = W_P C_{p,p} + W_w C_{p,w} \tag{3}$$

The thermal conductivity of the microcapsule was calculated using the composite sphere approach [9]:

$$\frac{1}{k_p d_p} = \frac{1}{k_c d_c} + \frac{d_p - d_c}{k_w d_p d_c} \tag{4}$$

The thermal conductivity of MPCS was calculated by Maxwell's relation [27]:

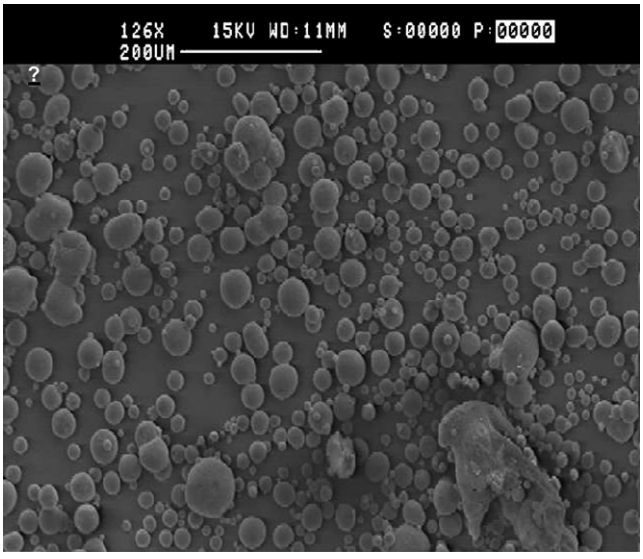


**Fig. 3.** SEM images of the microcapsules (DPNT06-0182 CIBA).

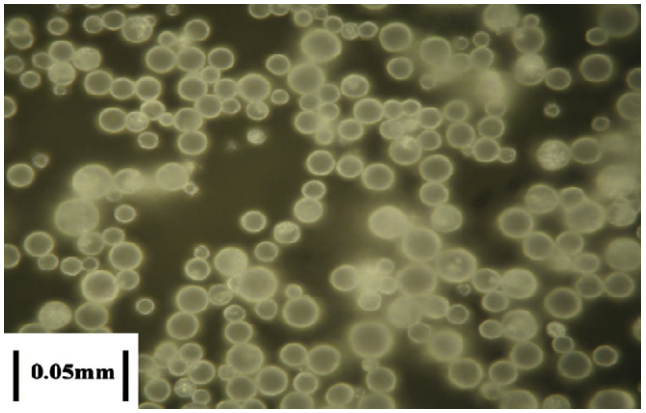


**Fig. 4.** Optical phase-contrast micrographs of the microcapsules (DPNT06-0182 CIBA).

$$k_b = \frac{2k_f + k_p + 2W\left(k_p - k_f\right)}{2k_f + k_p - W\left(k_p - k_f\right)} \tag{5}$$

### 2.6. Rheology measurement

Rheological properties were measured by a rheometer (Malvern Instruments–Kinexus Ultra). Three kinds of MPCS were prepared for each sample with the mass ratio of MPCM to water and surfactant: 10:90:1, 25:75:1, 35:65:1, respectively. The experiments were conducted at four different temperatures (below and above the melting temperature) for each MPCS.

## 3. Results and discussions

### 3.1. Microencapsulated phase change material

The FTIR spectra of the microcapsules (DPNT06-0182, CIBA) are presented in Fig. 1. The alkyl C–H stretching vibrations are found around 2900 $cm^{-1}$. C–H stretching peaks of crosslinked acrylic polymer are found around 1715 $cm^{-1}$. The peak at 1466 $cm^{-1}$ is due

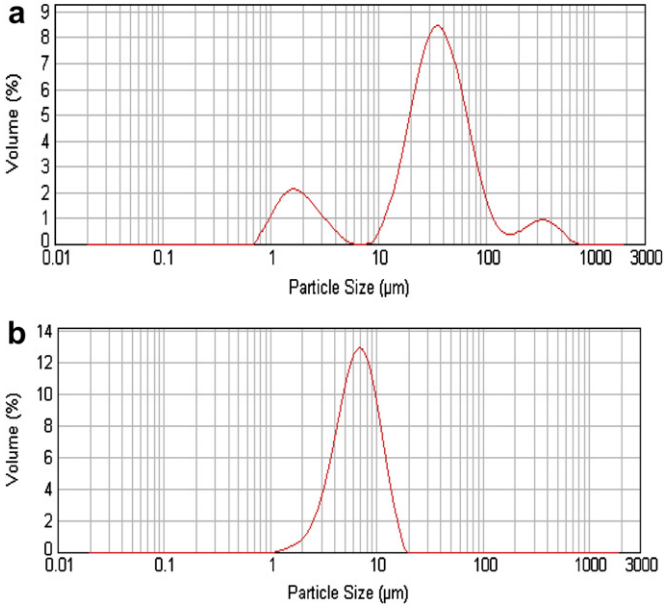


**Fig. 5.** (a). Particle size distribution of microcapsules (DPNT06-0182 CIBA). (b). Particle size distribution of microcapsules (DS 5008X BASF).

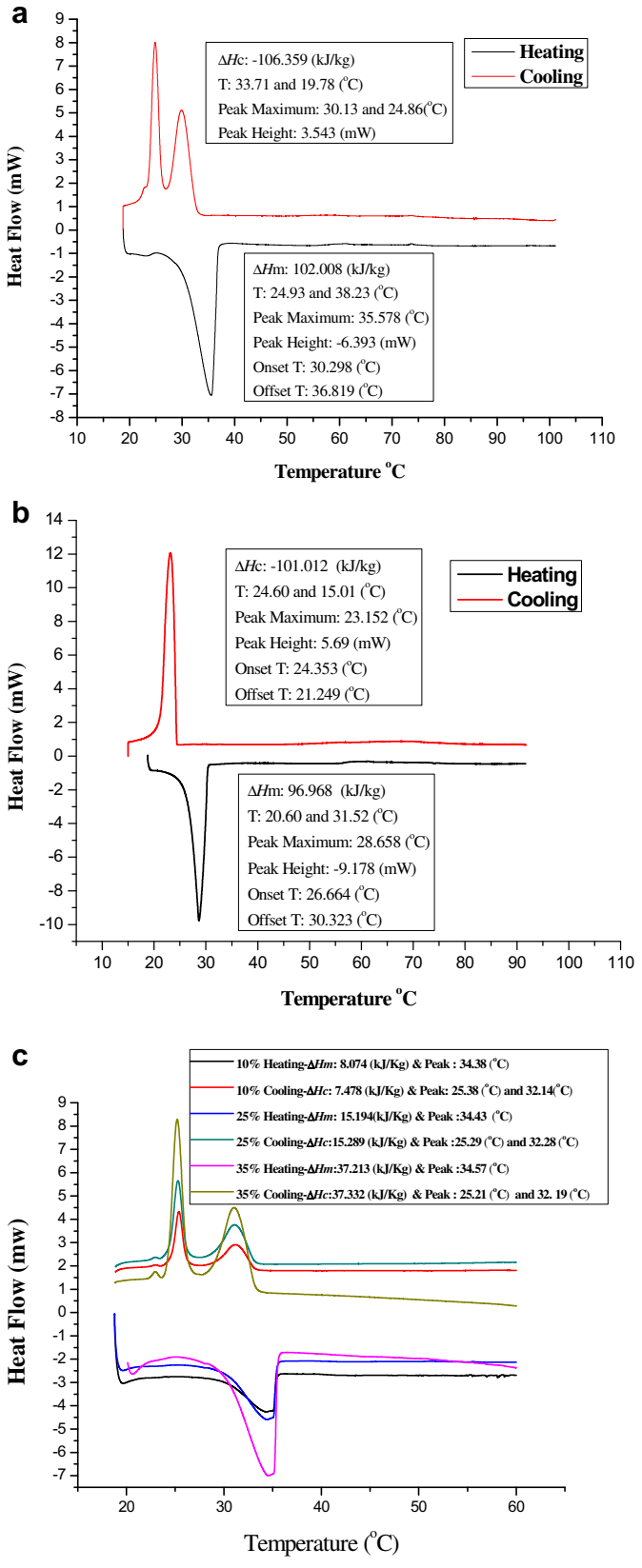


**Fig. 6.** (a). DSC curves of microencapsulated PCMs (DPNT06-0182 CIBA). (b). DSC curves of microencapsulated PCMs (DS 5008X). (c). DSC curves of microencapsulated PCS (10% wt., 25% wt., 35% wt.) (DPNT06-0182 CIBA).

to C–H bending and the peaks at 1170 cm $^{1}$ can be assigned to the C–O stretching of the ester group. FTIR spectra show both characteristic peaks of crosslinked acrylic polymer and paraffin wax. Fig. 2 shows the FTIR spectra of the microcapsules (DS 5008X BASF). The strong alkyl C–H stretching vibrations are found around 2950 cm . C–H stretching peaks of PMMA are found around 1730 cm . The peak at 1463 cm is due to C–H bending and the peaks at 1116 cm is associated with the C–O stretching of the ester group. The spectra of the microcapsules show both characteristic peaks of PMMA and paraffin mixture.

Fig. 3 shows the SEM images of the CIBA microcapsules with various diameters. The diameters of sample are in the range of 10–100 μm. It is observed that the most of the microcapsules have regularly spherical shape and smooth surface. The surfaces of the microcapsules are compact without any disfigurement on the shells of microcapsules. However, dimples exist on some of the microcapsules due to the volume contracting as paraffin crystallized. Similar SEM images of the BASF microcapsules are also examined (not shown here). Fig. 4 shows the optical phase-contrast micrographs of the CIBA microcapsules. An obvious core–shell microstructure can be distinguished from Fig. 4, where the bright circle layer representing the shell around the droplets is visible, and a core capsule of the paraffin mixture with dark color is obvious within the microcapsule. These microcapsules exhibit a regularly spherical shape without any obvious disfigurement on their surfaces. Zhang et al. [18] indicated that morphology of the microcapsules was greatly influenced by the stirring rate, emulsifier content during the fabrication process.

The particle size distribution (PSD) of the CIBA microcapsules is shown in Fig. 5(a). The PSD in volume shows multimodal distributions of particle sizes ranging in the interval between 0.7 and 700 μm. However, the most of particle sizes are in the size range from 10 to 100 μm. The average diameter of microcapsules was 40 μm. Fig. 5(b) shows the PSD of the BASF microcapsules, the agglomerated secondary particles of the powder can disintegrate under the effect of water. As it can see from Fig. 5(b), the PSD in volume shows unimodal distributions of particle sizes ranging from 1 to 20 μm and the average diameter of microcapsules was 7 μm. The stirring rate and emulsifier content have great effect on particle size distribution [18].

The thermal properties of the microcapsules of CIBA & BASF and the thermal properties of the MPCS of CIBA were measured by DSC, and their thermograms are presented in Fig. 6(a), (b) and (c), respectively, and the melting and crystallization properties of all samples are summarized in Table 1. It shows that there is only one peak appearing in the DSC heating thermograms for both samples. However, it is also found from Fig. 6(a) that two distinct peaks appear in the cooling thermograms of the CIBA microcapsules. Zhang et al. [45] indicated that the multiple peaks behavior on the DSC cooling curves are not caused by the difference of the cooling

**Table 1**
Thermal properties of the MPCMs and the MPCS.

| Sample name | $T_m$ (°C) | Δ $H_f$ (kJ/kg) | Onset $T_m$ (°C) | Offset $T_m$(°C) | $T_c$ (°C) α β | $\Delta H_c$ (kJ/kg) |
|---|---|---|---|---|---|---|
| CIBA sample | 35.578 | 102.008 | 30.298 | 36.819 | 30.1 24.9 | 106.359 |
| BASF sample | 28.658 | 96.968 | 26.664 | 30.323 | 23.152 | 101.012 |
| CIBA sample MPCS (10 wt %) | 34.38 | 8.074 | 29.967 | 35.34 | 32.1 25.4 | 7.478 |
| CIBA sample MPCS (25 wt %) | 34.43 | 15.194 | 30.438 | 35.402 | 32.3 25.3 | 15.289 |
| CIBA sample MPCS (35 wt %) | 34.57 | 37.213 | 29.919 | 35.496 | 32.2 25.2 | 37.332 |

rates in the measured range and they are mainly caused by the difference in the average diameter. A similar cooling behavior has been described for similar microencapsulated PCM systems in which the supercooling crystallization phenomena occurred when the diameter of microcapsules was smaller than 100 μm [12], the authors stated that during the crystallization of the paraffin mixture, the peak $\alpha$ is attributed to the heterogeneously nucleated liquid–rotator transition, which may be due to the crystallization of paraffin mixture on the inner wall of the microcapsules, and the peak $\beta$ is attributed to the homogeneously nucleated liquid–crystal transition. Yamagishi et al. [40] indicated that the supercooling crystallization was caused by the decrease in the number of nuclei in each microcapsule due to the reduced diameter. Fig. 6(c) shows that all three thermograms of the MPCS of CIBA samples present very similar melting temperature and crystallizing temperature to the MPCM of CIBA. However, the heat of fusion and the heat of crystallization of the MPCS were smaller than MPCM since the addition of water changes the latent heat storage capacity of MPCMs, and they are increasing gradually with the mass concentration of MPCS. Overall, the phase change properties of the microcapsules are mainly described with two important parameters, encapsulated efficiency ($\Phi$) and phase change temperature, $T_c$ and $T_m$. Especially, the heat of fusion of the microcapsules affecting

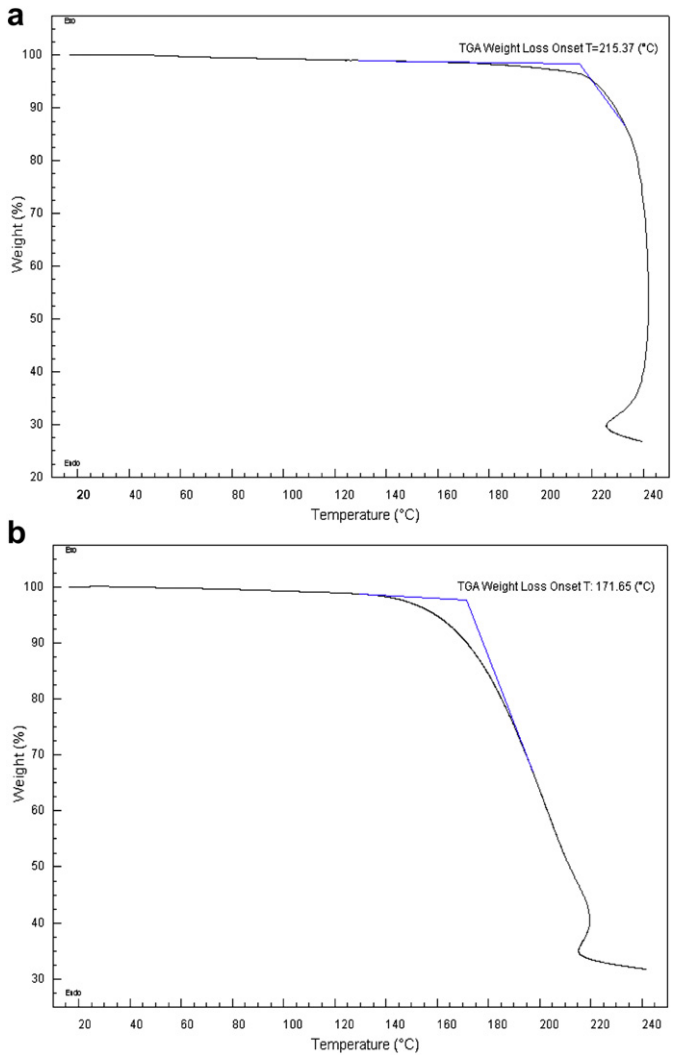


**Fig. 7.** (a). TG curves of microcapsules (DPNT06-0182 CIBA). (b). TG curves of microcapsules (DS 5008X).

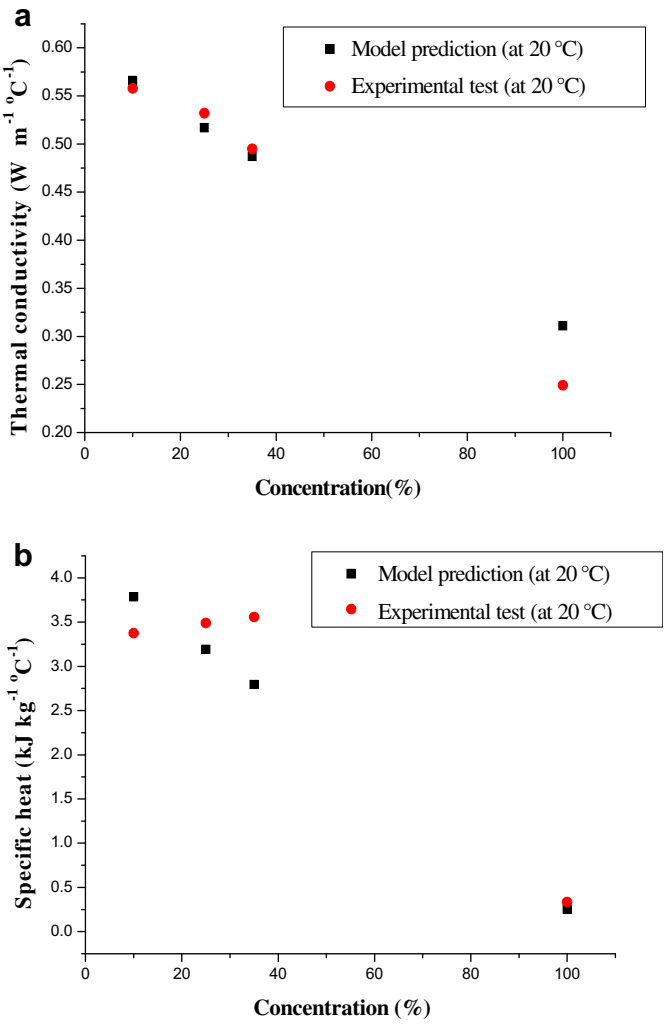


**Fig. 8.** (a). Effect of concentration on thermal conductivity (DPNT06-0182 CIBA). (b). Effect of concentration on specific heat (DPNT06-0182 CIBA).

the working effect of the MPCM that strongly depends on the encapsulated efficiency. Fig. 7(a) and (b) shows the weight loss percentage of the microcapsules with CIBA sample and BASF sample, respectively. It is notable that the CIBA sample has relatively better thermal stability than the BASF sample.

### 3.2. Microencapsulated phase change material slurries

Figs. 8 and 9 show the effect of concentration (wt %) on the thermal conductivity and the specific heat of the MPCS, respectively, for CIBA and BASF products. The results showed that the thermal conductivity and specific heat decreased with the increase of concentration due to the lower thermal conductivities and specific heat of the particles compared to the base fluid, water. Overall, the prediction agrees with the experimental data fairly well. It should be pointed out that the experimental test was carried out at the temperatures below the melting point of the PCMs inside the particles. For the case above the melting temperature of PCMs, the story may be different due to the phase change, and this warrants a further study for this problem in the future.

The rheological behaviors of the prepared MPCS with the mass concentration varying from 10%, 25% and 35% were measured by Kinexus Ultra Rheometer (Malvern Instruments Ltd), respectively. The results showed that the shear stress linearly increased with shear rate for 10% and 25% cases, therefore the slurry with

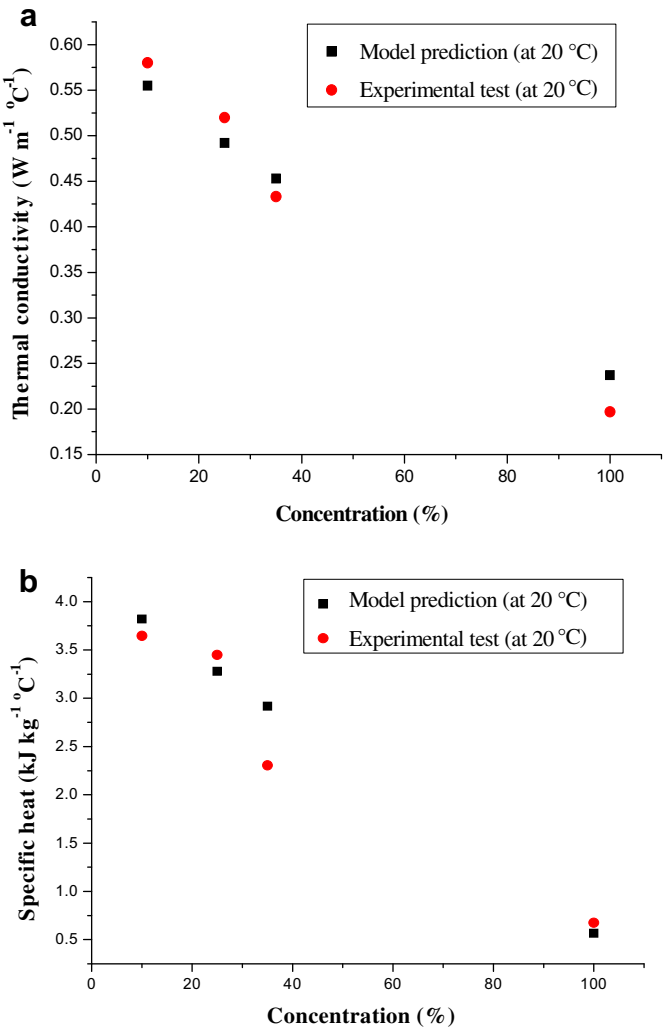


**Fig. 9.** (a). Effect of concentration on thermal conductivity (DS5008X BASF). (b). Effect of concentration on specific heat (DS5008X BASF).

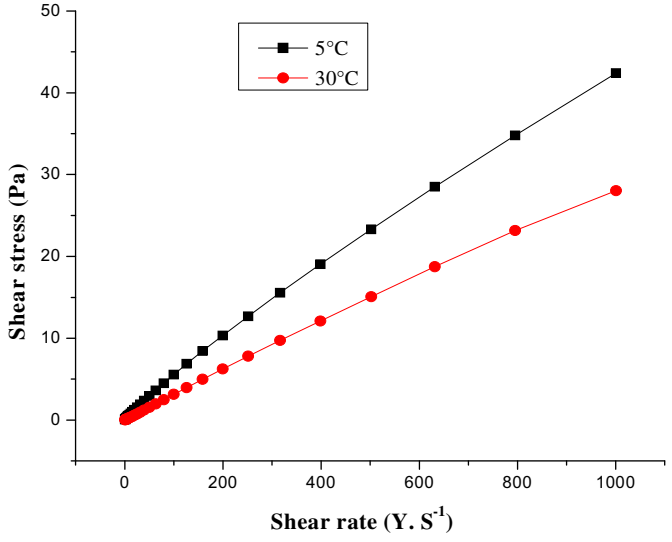


**Fig. 10.** Relationship of shear stress and shear rate at different temperatures for MPCS 25 wt.% (DS 5008X BASF).

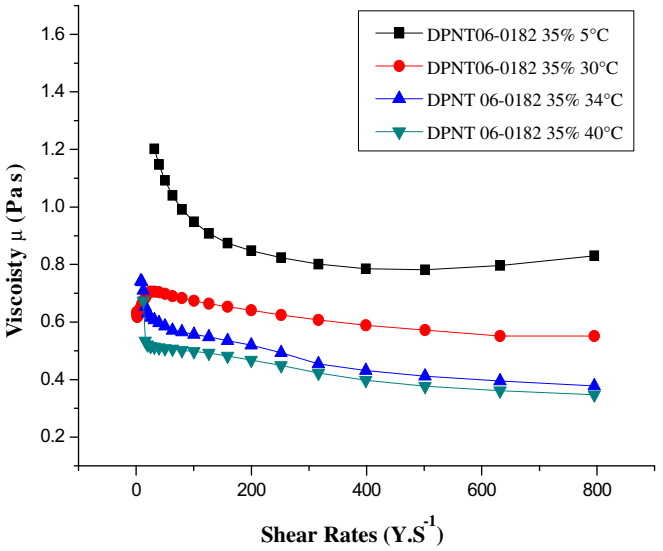


**Fig. 11.** The viscosities of MPCMs vs. shear rates (DPNT06-0182 CIBA 35%).

concentration below 25% can be considered as Newtonian fluid, and this well agrees with previous research by Charunyakorn et al. [46]. Fig. 10 shows the relationship of shear stress and shear rate for the MPCS of 25% at 5 °C and 30 °C, at which the PCMs are at solid phase and liquid phase, respectively. It is observed that the rheological behaviors will not be influenced by the PCM phase change process since the polymer shell of the microcapsules is always in contact with the carrying fluid (not the PCM content inside the shell). The dynamic viscosity of MPCS is very important for its flow behaviors. In this paper, the viscosities of samples at different temperatures and concentrations were measured by rheometer. Fig. 11 shows the viscosities of MPCMs vs. shear rates for the product of DPNT06-0182 CIBA at a given concentration 35% but at different temperatures. The viscosity decreases as the temperature rises, as expected. Also the viscosity exhibit a little shear thinning effect, namely, it decreases with increasing shear rate. Overall the MPCS can be considered as Newtonian fluid after 200 $s^{-1}$ shear rate, which is the minimal mean shear rate in the heat transfer experiment because the dynamic viscosity values are constant as the shear rates change. Fig. 12 shows the viscosity of slurries with different particle concentrations at a given temperature of 5 °C. As expected, the viscosity is higher with a higher concentration. Fig. 13

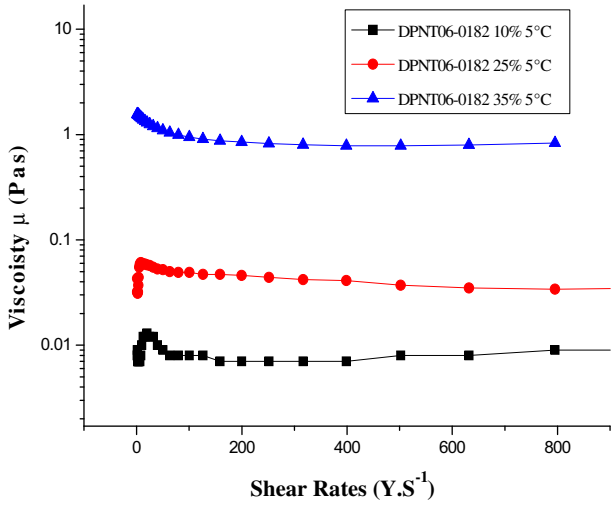


**Fig. 12.** The viscosities of MPCMs vs. shear rates (DPNT06-0182 CIBA at 5 °C).

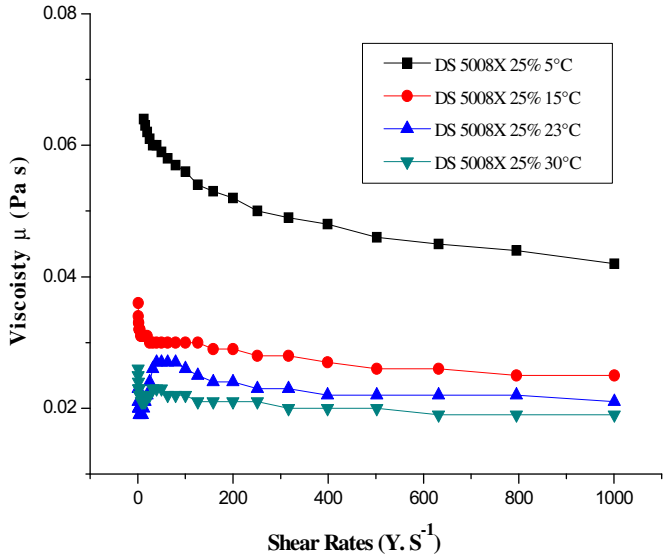


**Fig. 13.** The viscosities of MPCMs vs. shear rates (DS 5008X BASF 25%).

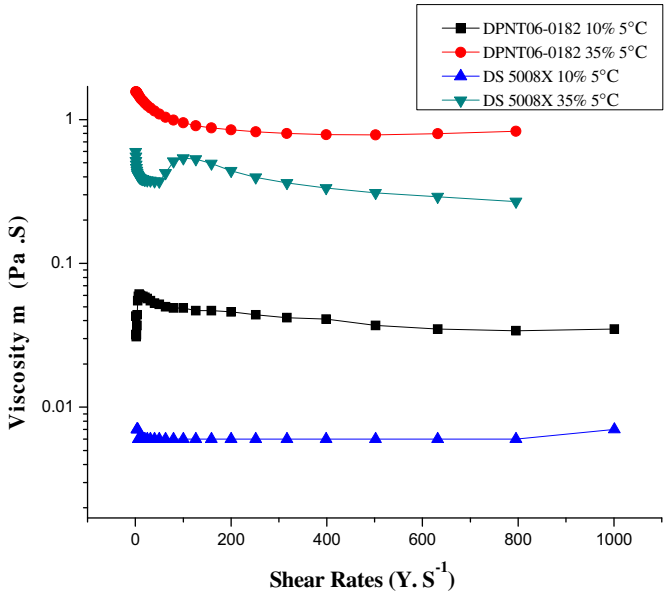


**Fig. 14.** The viscosities of MPCMs vs. shear rates (with different particle sizes).

presents the results for the product of DS 5008X BASF at concentration of 25%. Similar trend is observed. Fig. 14 examines the particle size effect on the viscosity of MPCS for a given particle concentration and a given test temperature. The results showed that the viscosity was higher for bigger particle slurries. Bearing in mind, the increase of viscosity will increase pump energy consumption, which will reduce the positive effect.

## 4. Conclusions

Experimental investigations have been carried out to investigate two different kinds of microencapsulated phase change materials (MPCMs) in terms of their thermal and rheological properties. The results showed that most of the microcapsules were spherical shaped and had smooth surfaces, and the structure analysis demonstrated that MPCMs had been successfully fabricated by their manufacturers. Particle size distribution (CIBA sample: 10–100 μm; BASF sample: 1–20 μm) was quite satisfactory for using these microcapsules in thermal energy storage and heat transfer. The heat of fusion of the two samples was 102 kJ/kg and 97 kJ/kg, respectively. Both samples showed very good thermal stability. Nevertheless, prevention of supercooling crystallization phenomena of MPCM still needs more intensive research, such as how to enhance the contents of materials in the fabrication process. In this paper, there were three kinds of MPCS were prepared for each sample with the mass ratio of MPCM to water and surfactant: 10:90:1, 25:75:1, 35:65:1, respectively. The addition of water did not change the melting temperature and crystallizing temperature of the MPCS samples. However, it changed the latent heat storage capacity of MPCMs and it increased gradually with the mass concentration of the MPCS. Overall the thermal conductivity and the specific heat of MPCS decreased with the particle concentration for the temperatures under the melting point. The dynamic viscosity of slurries decreased with the temperature rising. Overall the MPCS can be considered as Newtonian fluid within the test region (shear rate $>200\ s^{-1}$ and mass fraction $<0.35$). The viscosity was higher for bigger particle slurries. Finally, the results concluded that MPCMs that used in this study have good potential for thermal energy storage purposes and it could be used for solar space heating as well.

## Acknowledgment

This work is supported by the UK Engineering and Physical Science Research Council (EPSRC grant number: EP/F061439/1), the National Natural Science Foundation of China (Grant No: 51071184). The authors are thankful to the Ciba Specialty Chemicals, UK, and the BASF, Germany, for supplying samples. The authors are also thankful to the Birmingham Science City: Energy Efficiency and Demand Project (Project Ref: SY/SP8008).

## References

[1] Al-Jandal SS, Sayigh AAM. Thermal performance characteristics of STC system with phase change storage. Renewable Energy 1994;5:390–9.
[2] Hasan A, Sayigh AA. Some fatty acids as phase-change thermal energy storage materials. Renewable Energy 1994;4:69–76.
[3] Karaipekli A, Sarl A. Capric-myristic acid/expanded perlite composite as form-stable phase change material for latent heat thermal energy storage. Renewable Energy 2008;33:2599–605.
[4] Cai Y, Wei Q, Huang F, Lin S, Chen F, Gao W. Thermal stability, latent heat and flame retardant properties of the thermal energy storage phase change materials based on paraffin/high density polyethylene composites. Renewable Energy 2009;34:2117–23.
[5] Agyenim F, Eames P, Smyth M. Experimental study on the melting and solidification behaviour of a medium temperature phase change storage material (Erythritol) system augmented with fins to power a LiBr/$H_2O$ absorption cooling system. Renewable Energy 2011;36:108–17.
[6] Zhao CY, Lu W, Tian Y. Heat transfer enhancement for thermal energy storage using metal foams embedded within phase change materials (PCMs). Solar Energy 2010;84:1402–12.
[7] Zhao CY, Wu ZG. Heat transfer enhancement of high temperature thermal energy storage using metal foams and expanded graphite. Solar Energy Materials and Solar Cells 2011;95:636–43.
[8] Zhao CY, Zhou D, Wu ZG. Hear transfer enhancement of phase change materials (PCMs) in low and high temperature thermal storage by using porous materials. In: International Heat Transfer Conference-14, 8–13 August, 2010, Washington, D C, USA; 2010.
[9] Karaipekli A, Sarl A, Kaygusuz K. Thermal conductivity improvement of stearic acid using expanded graphite and carbon fiber for energy storage applications. Renewable Energy 2007;32:2201–10.
[10] Sarl A, Kaygusuz K. Some fatty acids used for latent heat storage: thermal stability and corrosion of metals with respect to thermal cycling. Renewable Energy 2003;28:939–48.
[11] Sharma A, Tyagi VV, Chen CR, Buddhi D. Review on thermal energy storage with phase change materials and applications. Renewable and Sustainable Energy Reviews 2009;13:318–45.
[12] Zhang H, Wang X. Fabrication and performances of microencapsulated phase change materials based on n-octadecane core and resorcinol-modified melamine-formaldehyde shell. Colloids and Surfaces A: Physicochemical and Engineering Aspects 2009;332:129–38.

[13] J Choi JL, Kim JH. H Yang Preparation of microcapsules containing phase change materials as heat transfer media by in-situ polymerization. Journal of Industrial and Engineering Chemistry 2001;7:358–62.
[14] Cho J-S, Kwon A, Cho C-G. Microencapsulation of octadecane as a phase-change material by interfacial polymerization in an emulsion system. Colloid & Polymer Science 2002;280:260–6.
[15] Hawlader MNA, Uddin MS, Zhu HJ. Encapsulated phase change materials for thermal energy storage: experiments and simulation. International Journal of Energy Research 2002;26:159–71.
[16] Hawlader MNA, Uddin MS, Khin MM. Microencapsulated PCM thermal-energy storage system. Applied Energy 2003;74:195–202.
[17] Fan YF, Zhang XX, Wang XC, Li J, Zhu QB. Super-cooling prevention of microencapsulated phase change material. Thermochimica Acta 2004;413: 1–6.
[18] Zhang XX, Fan YF, Tao XM, Yick KL. Fabrication and properties of microcapsules and nanocapsules containing n-octadecane. Materials Chemistry and Physics 2004;88:300–7.
[19] Kim EY, Kim HD. Preparation and properties of microencapsulated octadecane with waterborne polyurethane. Journal of Applied Polymer Science 2005;96: 1596–604.
[20] Tseng Y-H, Fang M-H, Tsai P-S, Yang Y-M. Preparation of microencapsulated phase-change materials (MCPCMs) by means of interfacial polycondensation. Journal of Microencapsulation 2005;22:37–46.
[21] Özonur Y, Mazman M, Paksoy HÖ, Evliya H. Microencapsulation of coco fatty acid mixture for thermal energy storage with phase change material. International Journal of Energy Research 2006;30:741–9.
[22] Alkan C, SarI A, Karaipekli A, Uzun O. Preparation, characterization, and thermal properties of microencapsulated phase change material for thermal energy storage. Solar Energy Materials and Solar Cells 2009;93:143–7.
[23] Yang R, Zhang Y, Wang X, Zhang Y, Zhang Q. Preparation of n-tetradecane-containing microcapsules with different shell materials by phase separation method. Solar Energy Materials and Solar Cells 2009;93:1817–22.
[24] Zhang GH, Zhao CY. Thermal and rheological properties of microencapsulated phase change material slurries. In: 5th International renewable energy storage conference IRES; 2010 [Invited Keynote paper, Berlin, Germany].
[25] Alkan C, SarI A, Karaipekli A. Preparation, thermal properties and thermal reliability of microencapsulated n-eicosane as novel phase change material for thermal energy storage. Energy Conversion and Management 2011;52: 687–92.
[26] SarI A, Alkan C, Karaipekli A. Preparation, characterization and thermal properties of PMMA/n-heptadecane microcapsules as novel solid-liquid microPCM for thermal energy storage. Applied Energy 2010;87:1529–34.
[27] SarI A, Alkan C, Karaipekli A, Uzun O. Microencapsulated n-octacosane as phase change material for thermal energy storage. Solar Energy 2009;83: 1757–63.
[28] Bryant YG. Melt Spun fibers containing microencapsulated phase change material Proceedings. ASME Symposium 1999;44:225–34.
[29] Zhang XX, Wang XC, Tao XM, Yick KL. Energy storage polymer/MicroPCMs blended chips and thermo-regulated fibers. Journal of Materials Science 2005; 40:3729–34.
[30] Sarier N, Onder E. The manufacture of microencapsulated phase change materials suitable for the design of thermally enhanced fabrics. Thermochimica Acta 2007;452:149–60.
[31] Onder E, Sarier N, Cimen E. Encapsulation of phase change materials by complex coacervation to improve thermal performances of woven fabrics. Thermochimica Acta 2008;467:63–72.
[32] Schossig P, Henning HM, Gschwander S, Haussmann T. Micro-encapsulated phase-change materials integrated into construction materials. Solar Energy Materials and Solar Cells 2005;89:297–306.
[33] Cabeza LF, Castellón C, Nogués M, Medrano M, Leppers R, Zubillaga O. Use of microencapsulated PCM in concrete walls for energy savings. Energy and Buildings 2007;39:113–9.
[34] Castellón C, Medrano PM, Roca PJ, Nogués PM, Castell A, Cabeza PLF. Use of microencapsulated phase change materials in building applications. Buildings 2007;X.
[35] Lee SH, Yoon SJ, Kim YG, Choi YC, Kim JH, Lee JG. Development of building materials by using micro-encapsulated phase change material. Korean Journal of Chemical Engineering 2007;24:332–5.
[36] Castellón C, Medrano M, Roca J, Cabeza LF, Navarro ME, Fernández AI, et al. Effect of microencapsulated phase change material in sandwich panels. Renewable Energy 2010;35:2370–4.
[37] Zhang P, Ma ZW, Wang RZ. An overview of phase change material slurries: MPCS and CHS. Renewable and Sustainable Energy Reviews 2010;14:598–614.
[38] Goel M, Roy SK, Sengupta S. Laminar forced convection heat transfer in microcapsulated phase change material suspensions. International Journal of Heat and Mass Transfer 1994;37:593–604.
[39] Roy SK, Avanic BL. Laminar forced convection heat transfer with phase change material emulsions. International Communications in Heat and Mass Transfer 1997;24:653–62.
[40] Yamagishi Y, Takeuchi H, Pyatenko AT, Kayukawa N. Characteristics of micro-encapsulated PCM slurry as a heat-transfer fluid. AIChE Journal 1999;45:696–707.
[41] Alvarado JL, Marsh C, Sohn C, Phetteplace G, Newell T. Thermal performance of microencapsulated phase change material slurry in turbulent flow under constant heat flux. International Journal of Heat and Mass Transfer 2007;50: 1938–52.
[42] Wang X, Niu J, van Paassen AHC. Raising evaporative cooling potentials using combined cooled ceiling and MPCM slurry storage. Energy and Buildings 2008;40:1691–8.
[43] Diaconu BM, Varga S, Oliveira AC. Experimental study of natural convection heat transfer in a microencapsulated phase change material slurry. Energy 2010;35:2688–93.
[44] Wang X, Niu J, Li Y, Wang X, Chen B, Zeng R, et al. Flow and heat transfer behaviors of phase change material slurries in a horizontal circular tube. International Journal of Heat and Mass Transfer 2007;50:2480–91.
[45] Zhang X-X, Fan Y-F, Tao X-M, Yick K-L. Crystallization and prevention of supercooling of microencapsulated n-alkanes. Journal of Colloid and Interface Science 2005;281:299–306.
[46] Charunyakorn P, Sengupta S, Roy SK. Forced convection heat transfer in microencapsulated phase change material slurries: flow in circular ducts. International Journal of Heat and Mass Transfer 1991;34:819–33.